

Josephson Current Suppression in Three-Dimensional Focussed Ion-Beam Fabrication of Sub-Micron Intrinsic Junctions

P. A. Warburton and J. C. Fenton

University College London, Dept. of Electrical and Electronic Engineering, Torrington Place, London, WC1E 7JE, UK.

M. Korsah and C. R. M. Grovenor

University of Oxford, Department of Materials, Parks Road, Oxford, OX1 3PH, UK.

This article was published as Supercond. Sci. Tech. (2006) 19 S187
<http://dx.doi.org/10.1088/0953-2048/19/5/S04>

ABSTRACT

We have fabricated intrinsic Josephson junction arrays in $\text{Tl}_2\text{Ba}_2\text{CaCu}_2\text{O}_8$ thin films using three-dimensional focussed ion-beam milling. We have measured the dependence of the switching current density of these arrays at 4.2 K upon the junction cross-sectional area. There is strong suppression of the switching current density for junctions of area less than $1 \mu\text{m}^2$, the current extrapolating to zero at an area of $0.25 \mu\text{m}^2$. We discuss the roles of gallium ion implantation and both thermal and quantum fluctuations in this current suppression.

INTRODUCTION

Since the spacing of consecutive copper-oxide double planes in many cuprate superconductors is greater than the coherence length in the *c*-direction, these planes are Josephson coupled. Hence a cuprate superconductor structure in which the current is forced to flow in the *c*-direction acts as a series array of “intrinsic” Josephson junctions [1]. Such junctions show promise for a wide variety of applications. For example, zero-crossing Shapiro steps at frequencies up to 2.5 THz have been measured in single crystal Bi-Sr-Ca-Cu-O intrinsic junctions [2], suggesting that they are suitable for development as voltage standards and sub-mm-wave oscillators. In addition there is a range of applications for sub-micron intrinsic junctions which exploit the Coulomb blockade effect, such as electric-field sensors and quantum current standards [3]. Intrinsic junctions are particularly suited to such applications since electron-electron interactions between neighbouring junctions (which are separated by ~ 1.7 nm) may lead to an enhancement of the charging energy, E_C , by a factor on the order of 10^3 [4, 5].

With such applications in mind, a variety of thin-film-based intrinsic junction device geometries has been proposed; for a review of such devices see [6]. We have developed a method for fabricating intrinsic Josephson junctions using three-dimensional focussed ion-beam milling [7, 8] of $\text{Tl}_2\text{Ba}_2\text{CaCu}_2\text{O}_8$ (TBCCO) thin films on lanthanum aluminate substrates. Such devices show high-quality underdamped (Stewart – McCumber parameter $\beta_c > 10^3$) current-voltage characteristics which are comparable to those obtained on single crystals. Here we show that the strong suppression of the apparent critical current for junctions of cross-sectional area A less than $1 \mu\text{m}^2$ may be the result of quantum fluctuations.

EXPERIMENTAL

Our device geometry, which makes use of c-axis oriented TBCCO films, is shown in Fig. 1. This structure is based on a similar device fabricated in Bi-Sr-Ca-Cu-O whiskers by Kim *et al.* [7]. The films, of typical thickness 600 nm, are grown on (0 0 1) oriented lanthanum aluminate single crystal substrates in a two-stage process. An amorphous sputtered Ba-Ca-Cu-O precursor is annealed *ex situ* in a thallos atmosphere at around 850 °C. The film is encapsulated by a sputtered gold film of approximate thickness 300 nm.

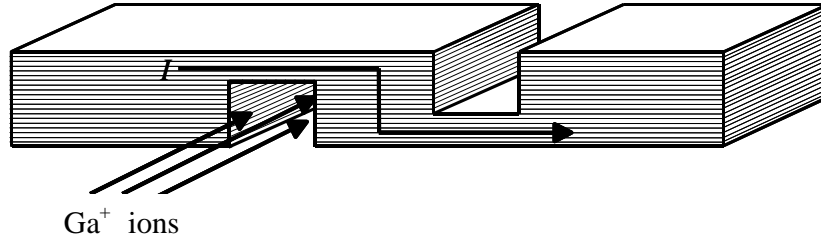


FIGURE 1: Schematic side view of our junction stacks. The narrow lines show (not to scale) the copper-oxide double-planes. Also shown is the transport current, I , and the orientation of the gallium ion beam during fabrication.

Gross patterning of the TBCCO lines which contact to the devices is done by using optical lithography and argon ion-milling. Tracks of typical width $w = 0.7 \mu\text{m}$ are then patterned in the film using normally-incident focussed ion-beam milling with a 30 keV gallium ion-beam. The substrate is then rotated so that the ion beam is almost parallel to it – in fact the angle between the beam and the substrate is typically 2° . This allows us to mill laterally the slots which force the current to flow parallel to the c-axis in the central part of the structure. Hence we have a stack of intrinsic junctions of cross-sectional area $A = wy$ and stack height z , which is expected to contain $N = (z / 1.7 \text{ nm})$ intrinsic junctions. A scanning electron micrograph of the final structure is shown in Fig. 2.

Four-point current-sourced measurements of the electronic properties of the devices are performed in a liquid helium storage vessel. Micro-coaxial cables and room-temperature low-pass filters are used to reduce external noise. Since in our sub-micron devices dissipation occurs at current bias levels less than the critical current, I_C , [9] we define an experimentally-measured switching current, I_{sw} , as the value of a quasi-static increasing current bias ramp at which the junction switches from the supercurrent branch to the first quasiparticle branch.

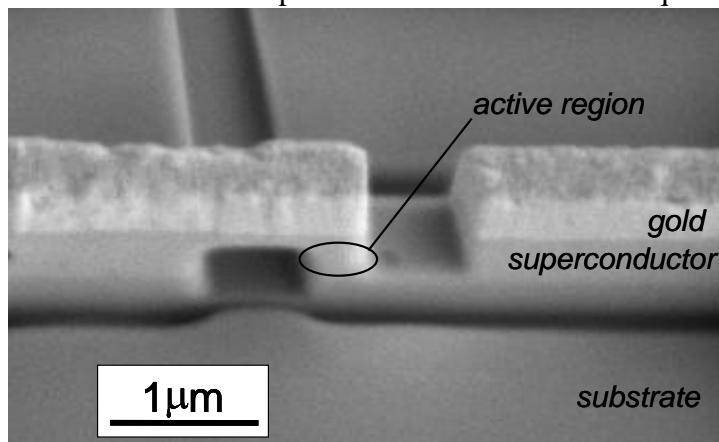


FIGURE 2: Scanning-electron micrograph showing the side view of a completed intrinsic junction stack. The superconductor is TBCCO.

RESULTS

All our devices show multi-branched current – voltage characteristics. A good example is shown in Fig. 3. There is a supercurrent branch at low (not always zero [9]) voltage and N quasiparticle branches. Here $N = 94 \pm 2$. This branched structure confirms the existence of a multitude of Josephson junctions in the array and is consistent with the height of the stack. The small value of the ratio of the retrapping current to the critical current shows that the Stewart – McCumber parameter, β_c , is large ($\sim 3 \times 10^3$). This in turn suggests that dissipation is low and comparable with the level of dissipation in intrinsic junctions based on single crystals.

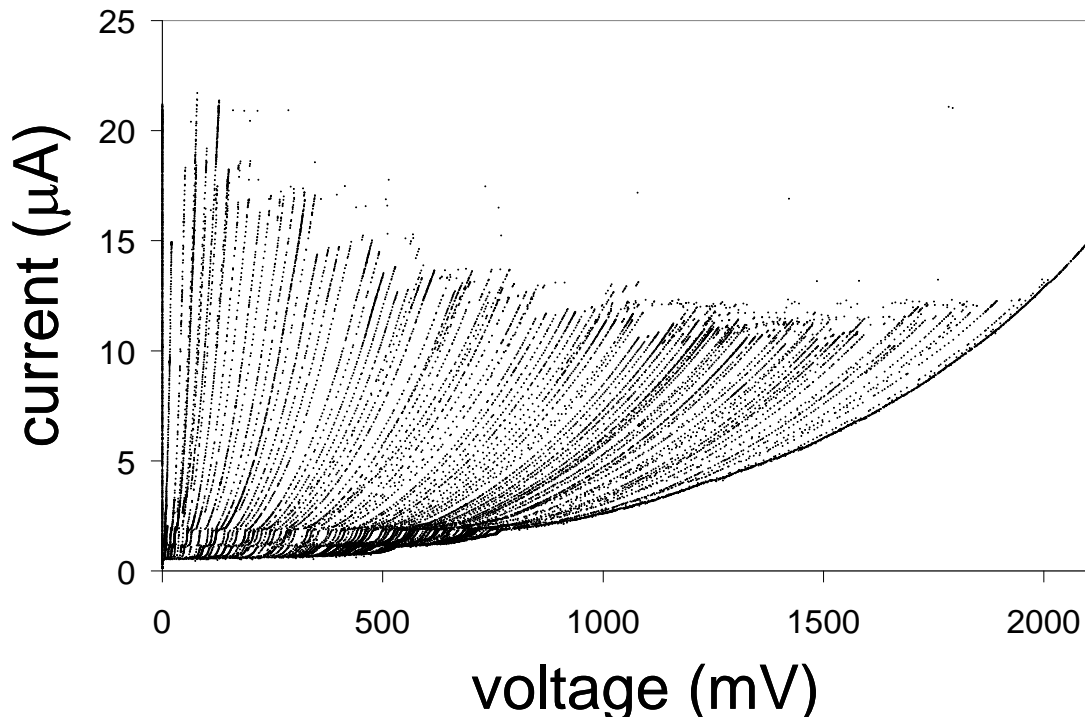


FIGURE 3: Four-point current-voltage characteristics of an intrinsic junction stack of cross-sectional area $0.7 \mu\text{m}^2$ at 4.2 K.

The dependence of the switching current, I_{sw} , and switching current density, $J_{sw} = I_{sw} / A$, measured at $T = 4.2$ K, upon the stack cross-sectional area, A , is shown in figure 4. For junction areas exceeding $1 \mu\text{m}^2$, J_{sw} is independent of A as expected, and approximately equal to 10^4 Acm^{-2} . This we take to be the unfluctuated value of the critical current, J_c , in our intrinsic junctions. For sub-micron junctions, however, the switching current is suppressed, extrapolating to zero at $A = 0.25 \mu\text{m}^2$.

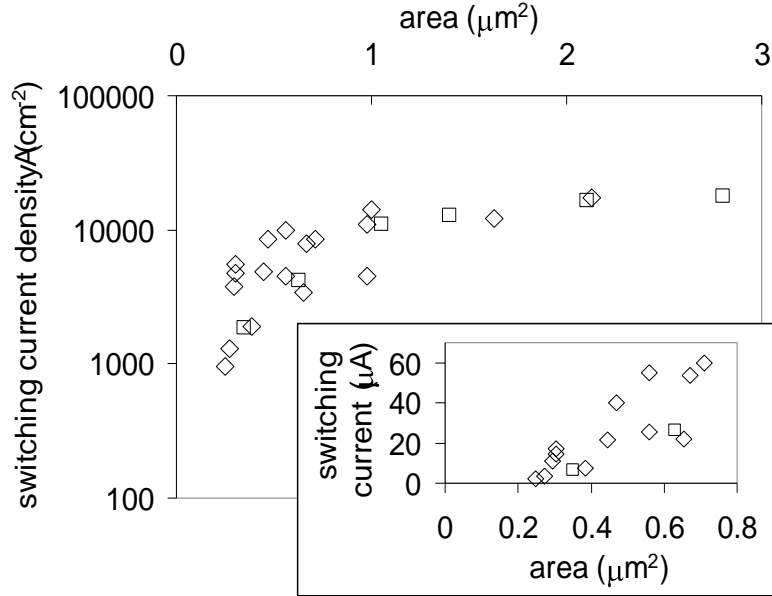


FIGURE 4: Area-dependence of the switching current density measured at 4.2 K (on a logarithmic axis) for a number of intrinsic junction stacks. Diamonds represent the devices fabricated using the technique discussed in this paper; squares represent devices fabricated on vicinal substrates (see [8]). The inset shows the area-dependence of the switching current for small junctions.

DISCUSSION

We now consider three mechanisms for this suppression of the switching current in sub-micron intrinsic junctions: gallium ion implantation, thermal fluctuations and quantum fluctuations.

Gallium Ion Implantation

During focussed ion-beam milling, gallium ions are implanted into all four sidewalls of our junction stack up to some distance d_{imp} . If we assume that these implanted regions do not contribute at all to conduction, the conductivity of a square junction stack should reduce to zero at $A_0 = 4 d_{imp}^2$. In order to experimentally estimate the value of d_{imp} we used gallium ion-milling to sequentially reduce the width, w , of a TBCCO thin film track of initial width 6 μm and measured its room temperature conductance. The dependence of this conductance upon the track width, w is shown in figure 5. The conductance extrapolates to zero at $w = 180$ nm. Since we milled both sides of the track, we infer that $d_{imp} = 90$ nm. Hence the “dead area” A_0 is equal to $0.032 \mu\text{m}^2$, which is an order of magnitude less than the area at which the switching current goes to zero (figure 4). We conclude that, while gallium implantation plays a role in suppressing conductivity in our devices, it cannot account fully for the switching current suppression we observe.

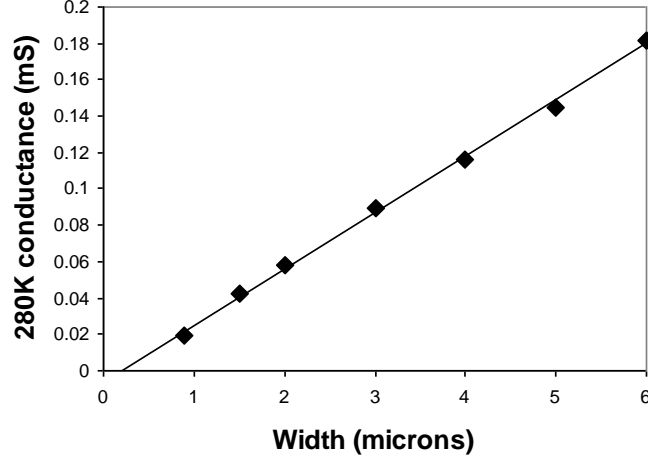


FIGURE 5: Width-dependence of the conductance of a TBCCO thin film track measured at 280 K. The line is a linear fit to the data.

Thermal Fluctuations

Even when the Josephson energy E_J is greater than kT , thermal fluctuations can cause premature switching from the supercurrent state to the quasiparticle branch [10, 11]. We have previously studied the role of thermal fluctuations on one of our sub-micron devices (of area $0.35 \mu\text{m}^2$) in some detail [9]. In this device the switching current at 4.2 K was $5.55 \mu\text{A}$. Under the assumption that switching was thermally-activated we inferred a critical current at $T = 0$ of $7.2 \mu\text{A}$ [9]. This suggests a critical current density of $2.1 \times 10^3 \text{Acm}^{-2}$, an order of magnitude less than that for our larger junctions. If we also include the effect of gallium implantation which reduces the effective area of the junction the critical current density is still only $3.2 \times 10^3 \text{Acm}^{-2}$. Thermal fluctuations and gallium implantation cannot therefore be the sole mechanisms for critical current suppression.

Quantum Fluctuations

In a *single* Josephson junction quantum fluctuations become significant when $\alpha = E_J / E_c$ is of order or less than 1. Here $E_J = \Phi_0 J_c A / (2\pi)$ is the Josephson coupling energy, $E_c = (2e)^2 / (2C)$ is the Coulomb energy, Φ_0 is the flux quantum, e the electronic charge and C the junction capacitance. For a *single* junction, therefore the condition $\alpha < 1$ is equivalent to

$$A < \left(\frac{4\pi e^2 d}{\Phi_0 J_c \epsilon_0 \epsilon_r} \right)^{1/2} \quad (1),$$

where d is the inter-cuprate-plane separation, ϵ_0 is the vacuum permittivity and ϵ_r the relative permittivity of the inter-plane barrier region. Taking $J_c = 10^4 \text{Acm}^{-2}$, $d = 1.4 \text{nm}$ and $\epsilon_r = 10$ we obtain $A < 0.005 \mu\text{m}^2$. On the face of it therefore one might expect junctions of the size and critical current density which we are discussing here to be unaffected by quantum fluctuations.

In arrays of N junctions, however, the charging energy can be enhanced by a factor N [4, 5, 12] due to inter-junction Coulomb interactions. One can expect this effect to be particularly marked in intrinsic junctions since the thickness of a cuprate double layer ($\sim 0.3 \text{nm}$) is not sufficient to completely screen the electric field. The case of a stack of N intrinsic junctions with strong Josephson coupling (*i.e.* $\alpha > 1$) has been analysed by Bulaevskii *et al.* [13]. They

show that quantum fluctuations cannot be neglected if $N > 2\alpha^{0.5}$. Hence for an array with 100 junctions quantum fluctuations are significant even if E_J is 10^3 times larger than E_c . Bulaevski *et al.* further go on to show that the critical current density when quantum fluctuations are taken into account takes the following functional form:

$$J_{c,qf} \approx J_c \exp\left(-\frac{N}{2\sqrt{\alpha}}\right) \quad (2).$$

Since $A \propto \sqrt{\alpha}$ we therefore replot the data of figure 4 in the form shown in figure 6 – *i.e.* $\log(J_{sw})$ versus $1/A_{eff}$. In this figure J_{sw} is calculated as I_{sw} / A_{eff} , where A_{eff} is the effective area of the junction, *i.e.* the actual physical area *less* the area of the perimeter which is gallium-implanted. There is plenty of scatter in the data, probably arising from the fact that we have poor experimental control over N . Nevertheless we do observe a trend which is not inconsistent with equation (2). From an exponential fit to the data in figure 6 we can extract the value of the critical current density in the absence of quantum fluctuations. If we take $N = 100$, we find $J_c = 6 \times 10^3 \text{ Acm}^{-2}$. This is in reasonable agreement with the measured J_c from larger junction stacks, given that the value of this estimate scales with N^2 , and here N varies from stack to stack.

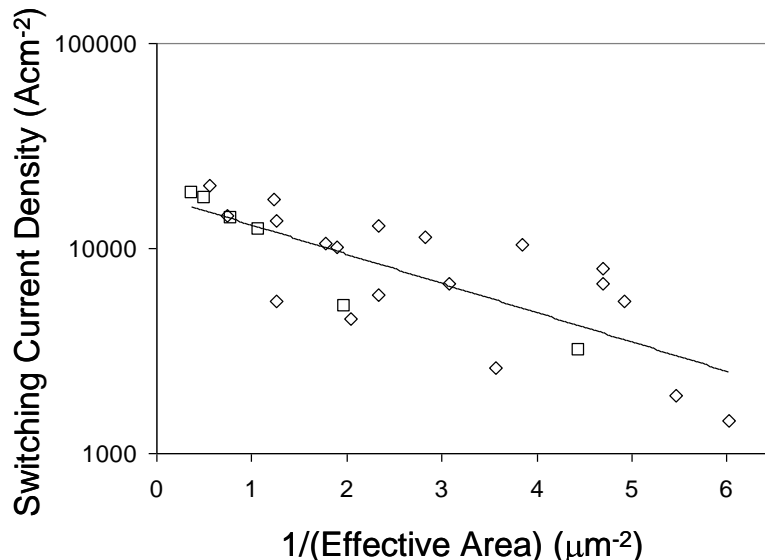


FIGURE 6: The dependence of the switching current density measured at 4.2 K (on a logarithmic scale) upon the inverse effective area. Diamonds represent the devices fabricated using the technique discussed in this paper; squares represent devices fabricated on vicinal substrates (see [8]). The line is an exponential fit to the data.

CONCLUSIONS

We have experimentally shown that the switching current density is suppressed below the critical current density in intrinsic Josephson junction stacks of cross-sectional area less than $1 \mu\text{m}^2$. On the basis of our experimental data it is difficult to be conclusive about the mechanism for this suppression, though it is clear that gallium ion-implantation and thermal fluctuations alone cannot account for it. The functional form of the area dependence of the switching current is not inconsistent with the predictions of Bulaevski *et al.* [13] who studied the role of quantum fluctuations on arrays of N intrinsic junctions in the regime $E_J / E_c \gg 1$. We need greater experimental control over N , which may be achieved by *in situ* monitoring of the array transport properties during ion milling [14], if we are to be more conclusive about the role of quantum fluctuations.

ACKNOWLEDGEMENTS

We acknowledge fruitful collaboration with Asan Kuzhakhmetov, Gavin Burnell, Chris Bell, Mark Blamire and Henrik Schneidewind. This work is funded by EPSRC.

REFERENCES

- [1] R. Kleiner *et al.*, "Intrinsic Josephson Effects In Bi₂Sr₂CaCu₂O₈ Single-Crystals," *Phys. Rev. Lett.* **68** 2394 (1992).
- [2] H. B. Wang *et al.*, "Terahertz responses of intrinsic Josephson junctions in high T- C superconductors," *Phys. Rev. Lett.* **87** 107002 (2001).
- [3] J. Bylander *et al.*, "Current measurement by real-time counting of single electrons," *Nature* **434** 361 (2005).
- [4] K. K. Likharev *et al.*, "Single-electron tunnel junction array: an electrostatic analog of the Josephson transmission line," *IEEE Trans. Mag.* **25** 1436 (1989).
- [5] K. K. Likharev and K. A. Matsuoka, "Electron-electron interaction in linear arrays of small tunnel junctions," *Appl. Phys. Lett.* **67** 3037 (1995).
- [6] A. A. Yurgens, "Intrinsic Josephson junctions: recent developments," *Supercond. Sci. Technol.* **13** R85 (2000).
- [7] S. J. Kim *et al.*, "Submicron stacked-junction fabrication from BSCCO whiskers by focused ion beam etching," *Appl. Phys. Lett.* **74** 1156 (1999).
- [8] P. A. Warburton *et al.*, "Sub-micron thin film intrinsic Josephson junctions," *IEEE Trans. Appl. Supercond.* **13** 821 (2003).
- [9] P. A. Warburton *et al.*, "Decoupling of a current-biased intrinsic Josephson junction from its environment," *Phys. Rev. B* **67** 184513 (2003).
- [10] M. Tinkham, *Introduction to Superconductivity*, Second Edition ed. New York: McGraw-Hill, 1996.
- [11] V. M. Krasnov *et al.*, "Probing the intrinsic Josephson coupling potential in Bi₂Sr₂CaCu₂O_{8+δ} superconductors by thermal activation," *Phys. Rev. B* **72** art. no. (2005).
- [12] D. B. Haviland *et al.*, "Superconducting and insulating behavior in one-dimensional Josephson junction arrays," *J. Low Temp. Phys.* **118** 733 (2000).
- [13] L. N. Bulaevskii *et al.*, "Quantum regime of Cooper pair tunneling in small-area Bi₂Sr₂CaCu₂O_{8+δ} mesas in magnetic fields," *Physica C-Superconductivity And Its Applications* **357** 418 (2001).
- [14] A. Yurgens *et al.*, "In situ controlled fabrication of stacks of high-T-c intrinsic Josephson junctions," *Appl. Phys. Lett.* **70** 1760 (1997).